Journal of Glaciology, Vol. 35, No. 119, 1989

SNOW-CRYSTAL GROWTH WITH VARYING SURFACE TEMPERATURES AND RADIATION PENETRATION

By S.C. COLBECK

(U.S. Army Cold Regions Research and Engineering Laboratory, Hanover, New Hampshire 03755-1290, U.S.A.)

ABSTRACT. The temperature field is derived for a sinusoidally varying surface temperature with varying solar radiation penetration. The growth rates of snow crystals are calculated to explain the rapidly growing layers of faceted crystals (i.e. depth hoar) that form just below the surface at high altitudes and in polar snow. The solutions also show that a layer of wet snow can exist just below the surface even on days when the surface temperature remains sub-freezing.

INTRODUCTION

Most studies of seasonal snow covers have concentrated on the basal layers because of the inherent interest in the formation of depth hoar and because of the difficulties of dealing with the complicated processes that occur near the surface. Depth hoar is an extreme example of the faceted crystals which grow in snow when the snow is subjected to a large temperature gradient. These crystals have long been of interest in avalanche studies because of the possibility that slab avalanches are released as a result of low strength in these buried layers. Faceted crystals are also produced in the uppermost snow layers of the polar ice sheets (Schytt, 1958), where they have long been associated with "firn quakes", a sudden collapse of a sub-surface layer which is detectable over some distance. These annually generated layers have also proved useful as marker horizons (Gow, 1965).

While the temperature gradient in a basal layer may be nearly constant, there are wide swings in the temperature gradient near the surface because of the large diurnal variations in temperature and solar radiation at the surface of most seasonal snow covers. In polar snow these variations occur annually.

There are two interesting effects from these surface boundary conditions. First, sub-surface melting is sometimes observed in a snow cover by radar observation when the surface temperature is below the melting temperature (personal communication from R. Berger, U.S. Army CRREL). The absoption of radar energy is relatively high when melt water is present, so the possibility of sub-surface melting by penetrating solar radiation is of some consequence to the interpretation of radar back-scatter from snow covers. Secondly, as mentioned above, the formation of faceted crystals of the depth-hoar type occurs most often in the basal layers of snow covers but also just below the surface in both seasonal and polar snows. In seasonal snow, this phenomenon occurs at high elevations where the solar radiation is strongest. In places, the formation of these layers is thought to be responsible for avalanche release once the weak layer of faceted crystals is buried by subsequent snowfalls (LaChapelle, 1970; Akitaya and Shimizu, 1987).

In polar snow, the observation of highly faceted crystals seems most unusual because the temperature gradient away from the annual cycle is much too small to explain their growth. Thus, the strong temperature gradients produced by the annual or diurnal temperature cycles must explain the rapid growth of crystals near the surface. To explain this near-surface growth, I begin by developing the theory of spatial and temporal variations in temperature with sinusoidally varying surface temperature and periodic solar radiation at the surface. The calculated temperature and temperature-gradient profiles are used to find the profile of crystal growth to examine the near-surface growth of faceted crystals.

THEORY

The propagation of temperature transients into a half-space because of periodically varying surface temperatures, but without radiation penetration, has been described by Carslaw and Jaeger (1959, p. 64). When solar radiation is penetrating the surface and being absorbed in the snow, there is an energy source which raises the temperature (T) according to

$$\rho c \frac{\partial T}{\partial t} = k \frac{\partial^2 T}{\partial z^2} + \lambda I(t) e^{-\lambda z} \qquad (1)$$

where ρ is the snow density, c is its specific heat, t is time, k is the thermal conductivity of snow, λ is the radiation absorption constant, $I(t)$ is the radiation penetrating the surface (after surface reflection), and z is the depth below the surface. To solve this equation, I let

$$u = T - \lambda e^{-\lambda z} A(t) - \bar{T}(0) \qquad (2)$$

where $A(t)$ is an arbitrary function of time, $\bar{T}(0)$ is the temporally averaged surface temperature, and u satisfies the equation

$$\rho c \frac{\partial u}{\partial t} = k \frac{\partial^2 u}{\partial z^2}. \qquad (3)$$

It follows that A satisfies

$$A(t) = A(0) e^{\alpha t} + \frac{e^{\alpha t}}{\rho c} \int_0^t I(t) e^{-\alpha t} dt \qquad (4)$$

where α is defined by

$$\alpha = k\lambda^2 / \rho c. \qquad (5)$$

The solution of u with the appropriate boundary condition must now be sought.

A good approximation to the radiation boundary condition of interest as shown in Figure 1 is given by

$$I(t) = \frac{b}{\pi} + \frac{b}{2} \sin \omega t - \frac{2b}{3\pi} \cos 2\omega t \qquad (6)$$

https://doi.org/10.3189/002214389793701536 Published online by Cambridge University Press

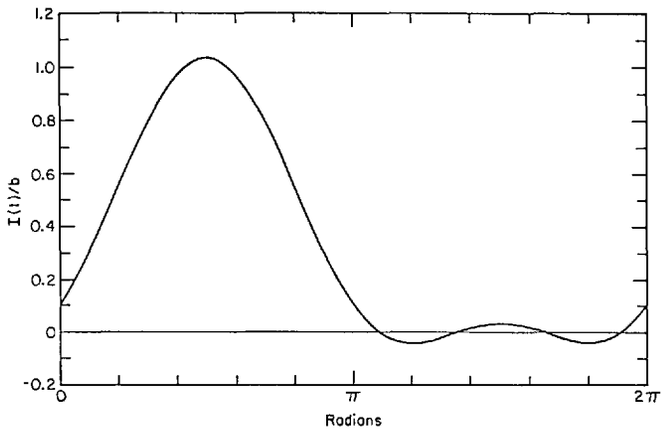

Fig. 1. Assumed form of penetrating solar radiation as given by Equation (6). Note that the cycle starts at sunrise.

where b is approximately equal to the peak of the radiation that penetrates the snow surface and ω is the frequency. I assume a value for $A(0)$ that eliminates $e^{\alpha t}$ in Equation (4); then the boundary condition for u is

$$u(0,t) = a\sin(\omega t - \varepsilon) + \tag{7}$$

$$+ \frac{\lambda b}{\rho c}\left[\frac{1}{\alpha\pi} + \frac{\alpha\sin\omega t + \omega\cos\omega t}{2(\alpha^2 + \omega^2)} + \right.$$

$$\left. + \frac{2}{3\pi}\frac{2\omega\sin 2\omega t - \alpha\cos 2\omega t}{\alpha^2 + 4\omega^2}\right]$$

where the first term comes from the thermal boundary condition,

$$T(0,t) = a\sin(\omega t - \varepsilon) + \bar{T}(0) \tag{8}$$

where a is the amplitude of the surface-temperature fluctuation, and ε is the phase lag between $\pi/2$ and the time of maximum surface temperature. I include ε because the surface-temperature peak normally lags the radiation peak. No surface-energy fluxes were used to determine this boundary condition but rather it is simply assumed as a reasonable approximation to the usual situation.

The solution for u for this boundary condition is obtained from the solution method for $u(z,0)$ equals zero given in Carslaw and Jaeger (1959, p. 63); then the solution for T is obtained by reversing the transformation involving u. If the average temperature profile $\bar{T}(z)$ was originally non-zero, it has been transformed to zero by the solution method and it is necessary to add it back into the solution. Another way of thinking about this is that, if the temporally averaged temperature gradient is not zero, the temperature variable should be transformed such that the gradient is zero, the partial differential equation solved in the new variable, and then transformed back to the actual temperature. The result is

where κ is the thermal diffusivity, or $k/\rho c$. There are additional terms of a transient nature in Equation (9) which have been ignored because only the periodic solution is of interest. The erfc term is also a transient term which must be accepted because it would change the nature of the solution if ignored. It arises because the penetration of solar radiation would heat the snow by an amount equal to $b/k\lambda\pi$ at infinite time. This would happen much faster if it were not for the steep temperature gradients associated with a sinusoidal surface temperature. Ignoring the other transients merely means that the solution is examined after a sufficient number of cycles have passed to remove the effects of those transients. However, the energy available from radiation penetration is substantial compared to the thermal mass of the snow, so this effect is examined in more detail.

Since the initial temperature profile was not specified, it occurs as dictated by the assumption that $u(z,0)$ equals zero. The profiles up to 100 cycles are shown in Figure 2 where it can be seen that, after the first cycle, the solution

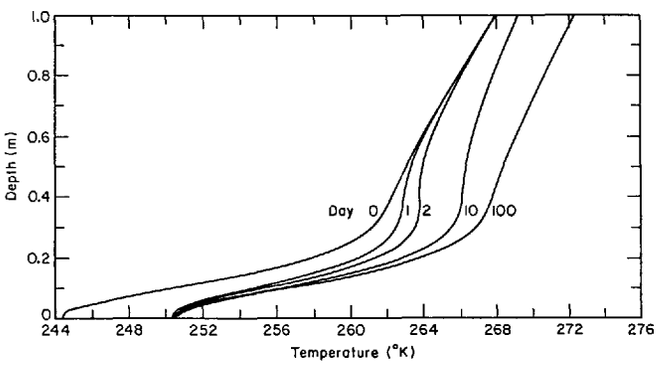

Fig. 2. Temperature profiles after repeated cycles of surface temperature and solar radiation (see Table I for the parameters used in each example).

changes rather slowly with time. The sub-surface temperature does increase with time because of the accumulated radiation but the transient part of the solution is not large enough to be a significant factor overall. I can ignore it and still draw valid conclusions from the second cycle, 2π to 4π. For infinitely many cycles, the erfc term would shift the entire solution to warmer temperatures by $b/k\lambda\pi$, or 6.4 °C for the example given in Figure 2. However, if only a small part of 1 d were cloudy, the cumulative effect of the erfc term could be eliminated by the heat flow associated with the mean temperature gradient.

A test of the solution is given in Figure 3 for two values of the radiation parameter, b. Figure 3a shows the symmetrical solution for no radiation input and the sinusoidal boundary condition. Figure 3b shows the skewed solution for a large input of radiation. Clearly, the radiation input shifts the temperatures near the surface to higher values and changes the nature of the temperature gradients. These computed profiles are skewed in the same direction as Weller and Schwerdtfeger's (1977) measured values at Plateau Station in Antarctica. The temperature just below

$$T(z,t) = \bar{T}(z) + \frac{b}{k\lambda\pi}\operatorname{erfc}\frac{z}{2(\kappa t)^{\frac{1}{2}}} + \tag{9}$$

$$+ ae^{-z(\omega/2\kappa)^{\frac{1}{2}}}\sin(\omega t - \varepsilon - z(\omega/2\kappa)^{\frac{1}{2}}) -$$

$$- \frac{b\lambda}{\rho c}e^{-\lambda z}\left[\frac{1}{\alpha\pi} + \frac{\alpha\sin\omega t + \omega\cos\omega t}{2(\alpha^2 + \omega^2)} + \frac{2}{3\pi}\frac{2\omega\sin 2\omega t - \alpha\cos 2\omega t}{\alpha^2 + 4\omega^2}\right] +$$

$$+ \frac{b\lambda e^{-z(\omega/2\kappa)^{\frac{1}{2}}}}{2\rho c(\alpha^2 + \omega^2)}\left[\alpha\sin(\omega t - z(\omega/2k)^{\frac{1}{2}}) + \omega\cos(\omega t - z(\omega/2\kappa)^{\frac{1}{2}})\right] +$$

$$+ \frac{2b\lambda e^{-z(\omega/\kappa)^{\frac{1}{2}}}}{3\pi\rho c(\omega^2 + 4\omega^2)}\left[2\omega\sin(2\omega t - z(\omega/\kappa)^{\frac{1}{2}}) - \alpha\cos(2\omega t - z(\omega/\kappa)^{\frac{1}{2}})\right]$$

https://doi.org/10.3189/002214389793701536 Published online by Cambridge University Press

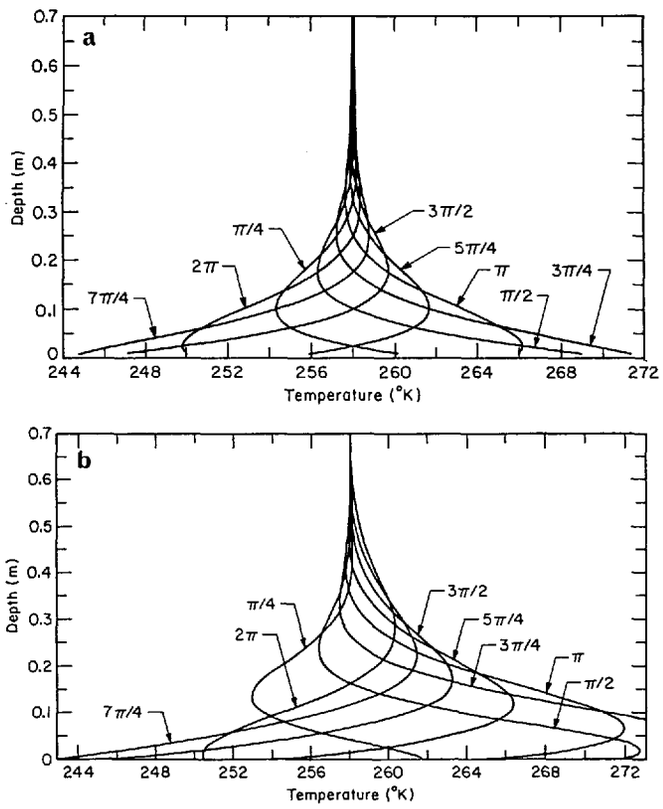

Fig. 3. Temperature profiles for no solar input (a) and a strong solar input (b). Notice that there would be sub-surface melting during part of the cycle with solar input.

the surface reaches the melting temperature for a short period in this example. The solution is not strictly correct since Equation (1) did not include melting. However, the effect is rather small because of the limited amount of melting taking place. This highly skewed solution does show that sub-surface melting can occur during periods when the surface is entirely sub-freezing. However, I cannot explore the full range of possibilities without expanding Equation (1) to include phase change.

The temperature gradient which drives the vapor flux and therefore controls crystal growth must also be calculated. It is derived from Equation (9) as

The temperature-gradient profiles over one cycle are shown in Figure 4 for the same parameters as those used in Figure 3b. These gradients are also skewed because of solar heating over just part of the cycle. If it were not for

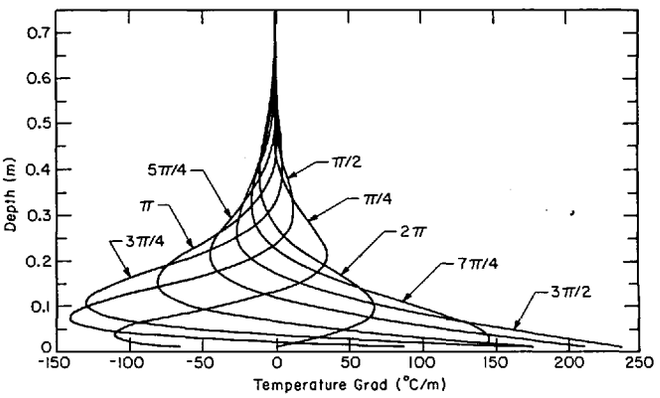

Fig. 4. Temperature-gradient profiles with strong solar-radiation input.

these highly skewed gradients, the erfc term would have a much greater effect than shown in Figure 2. There is also a transient term in Equation (10), the derivative of the erfc term in Equation (9), but it is negligible after the first cycle.

EXAMPLES

Three specific examples — a seasonal snow cover, a high-altitude snow cover, and polar ice-sheet snow — are given to illustrate the effects of radiation penetration on the temperature field and grain growth in snow. These three have significantly different conditions of radiation input, average temperature, and temperature extremes.

Seasonal snow cover

I assume a 1 m depth with a 30 K temperature swing in clear weather with strong radiational input during the day. If the snow–soil contact is at 0 °C, the daily average temperature for various values of incoming solar radiation is shown in Figure 5. A likely value for b in a mid-latitude snow cover is about 70 W/m², which indicates a temperature rise of about 3 °C at 0.15 m depth due to penetrating solar radiation.

$$T' = \bar{T}'(z) + \frac{b\lambda^2 e^{-\lambda z}}{\rho c}\left[\frac{1}{\alpha\pi} + \frac{\alpha\sin\omega t + \omega\cos\omega t}{2(\alpha^2+\omega^2)} + \right.$$

$$+ \frac{2}{3\pi}\frac{2\omega\sin 2\omega t - \alpha\cos 2\omega t}{\alpha^2+4\omega^2} - \qquad (10)$$

$$+ \frac{b\lambda(\omega/2\kappa)^{\frac{1}{2}}e^{-z(\omega/2\kappa)^{\frac{1}{2}}}}{2\rho c(\alpha^2+\omega^2)}\left[(\omega-\alpha)\sin(\omega t - z(\omega/2\kappa)^{\frac{1}{2}}) - \right.$$

$$\left. - (\omega+\alpha)\cos(\omega t - z(\omega/2\kappa)^{\frac{1}{2}})\right] -$$

$$- \frac{b}{\kappa\lambda\pi^{3/2}}e^{-z^2/4\kappa t}\frac{1}{(\kappa t)^{\frac{1}{2}}} - \alpha(\omega/2k)^{\frac{1}{2}}e^{-z(\omega/2\kappa)^{\frac{1}{2}}}\left[\sin(\omega t - \varepsilon - z(\omega/2\kappa)^{\frac{1}{2}}) + \right.$$

$$\left. + \cos(\omega t - \varepsilon - z(\omega/2\kappa)^{\frac{1}{2}})\right] +$$

$$- \frac{2b\lambda(\omega/\kappa)^{\frac{1}{2}}e^{-z(\omega/\kappa)^{\frac{1}{2}}}}{3\pi\rho c(\alpha^2+4\omega^2)}\left[(2\omega-\alpha)\cos(2\omega t - z(\omega/\kappa)^{\frac{1}{2}}) + \right.$$

$$\left. + (2\omega+\alpha)\sin(2\omega t - z(\omega/\kappa)^{\frac{1}{2}})\right].$$

https://doi.org/10.3189/002214389793701536 Published online by Cambridge University Press

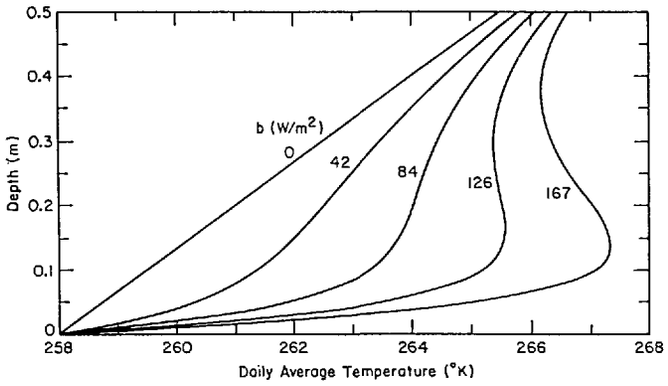

Fig. 5. Average daily temperature profiles for various solar inputs and a strong background temperature gradient.

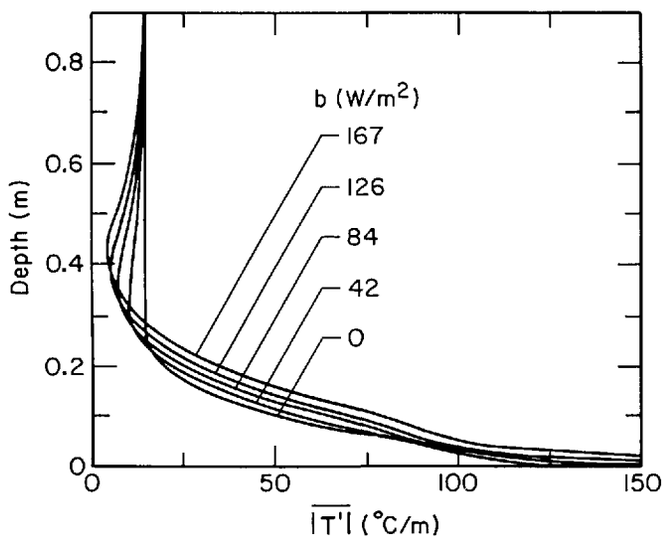

Fig. 6. Profiles of the daily average of the absolute value of the temperature gradient for various values of solar input.

The average value of the absolute temperature gradien for different amounts of radiation is shown in Figure 6. The absolute value is used because it is a measure of crystal growth due to vapor flow, either upward or downward. It seems from Figure 6 that the magnitude of the penetrating radiation does not have too much effect on the average of the absolute value of the temperature gradient, or therefore, on vapor flow. In fact, it appears that the vapor flow would decrease below about 0.25 m as the radiation input increases. However, from the surface down to about 0.25 m, the growth rate would increase with increasing radiation. Nevertheless, it may be that the faceted crystals that grow just below the surface are caused mostly by diurnal temperature cycles, and not by radiation penetration. Usually, the strongest diurnal temperature cycles occur during periods of clear weather, so the two usually occur together. The effect of temperature cycling is given in Figure 7 where profiles of the average value of the absolute temperature gradient are shown for various values of a, the amplitude of the surface-temperature cycle. Near the surface, the vapor would increase significantly with the value of a, but there would be some vapor flow due to the cyclic radiation input, even if there were no surface-temperature oscillation. Thus, either radiation absorption or surface-temperature cycling could cause an acceleration in crystal growth just below the surface.

To examine this question further, I will consider the combined effects of temperature and temperature gradient on crystal growth. The temperature gradients are larger near the surface but the temperature itself is often lower there and both affect the rate of crystal growth. The temperature gradient is critical to understanding the growth of crystals because they grow by a process that has been characterized as the "hand-to-hand delivery of water vapor", or the exchange of vapor among neighboring ice crystals of

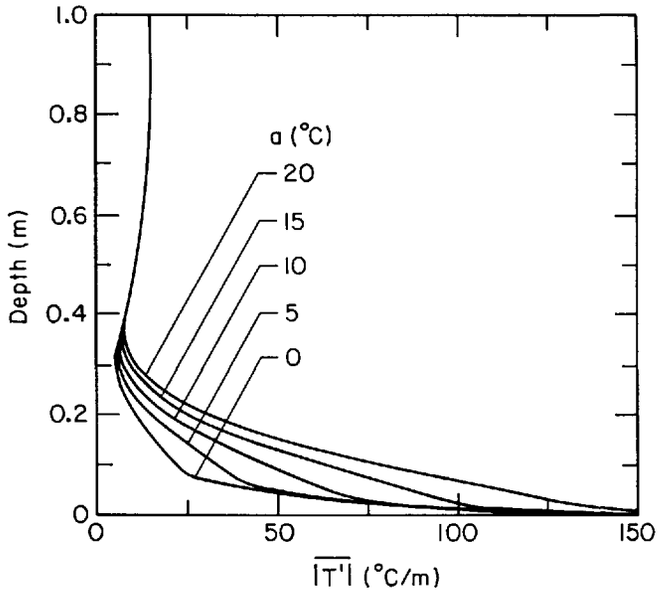

Fig. 7. Profiles of the daily average of the absolute value of the temperature gradient for various values of the amplitude (a) of the surface-temperature variation.

different temperatures. When a temperature gradient exists in the snow cover, that gradient causes heat and vapor flow in the direction of lower temperatures, both processes being greatly affected by the presence of the crystals. In the case of vapor flow, the flow tends to be between adjacent crystals with vapor moving from the warmer side of an air space to the colder side. If natural convection occurs, that also must be considered (Powers and others, 1985), but it is not common.

The temperature is also important because it has a large effect on the rate of growth of ice crystals. These ideas are included in a model of the process (Colbeck, 1983), where the growth rate is given by

$$\dot{m} = 2\pi CD\left[z\Delta\sigma + \frac{1}{\beta} - \left[\frac{4\Delta\sigma}{\beta} + \frac{1}{\beta^2}\right]^{\frac{1}{2}}\right] \qquad (11)$$

where C is a shape factor that depends on particle size, shape, and separation, D is the coefficient of diffusion of water vapor in air, $\Delta\sigma$ is given by

$$\Delta\sigma = g|T'|\mathrm{d}\sigma/\mathrm{d}T \qquad (12)$$

where g is a factor which accentuates the effect of temperature differences due to local heat-flow paths, σ is vapor density at ice saturation, and β is given by

$$\beta = c\tau A/4\pi CD \qquad (13)$$

where c is a constant, A is the surface area of the growing crystal, and τ is the temperature-dependence of crystal growth found by Lamb and Hobbs (1971). Again, the sign of the temperature gradient is ignored because vapor flowing either upwards or downwards would cause crystal growth. To put τ in functional form, I assume an approximation

$$\tau = 136e^{0.340T_r} \qquad (14)$$

where $2r$ is the size of the crystal. Equation (14) is a good approximation but it does not include the two rises in the original data that are associated with changes in the dominant crystal type. There are other problems with using this approach as well since, for a simple geometrical arrangement of crystals in snow, the vapor pressure over the growing crystals seems too high near the surface, as described by Colbeck (1983). There it was shown that the solution to this problem is simply to treat the geometrical snow parameters as statistically distributed, but that it not necessary here because only the growth is calculated.

https://doi.org/10.3189/002214389793701536 Published online by Cambridge University Press

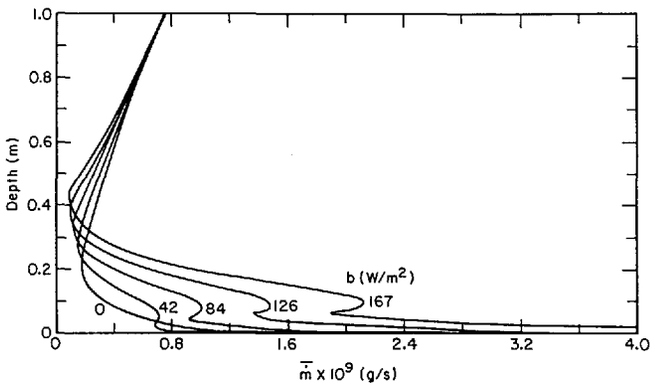

Fig. 8. Profiles of the daily average of the crystal-growth rate for various values of the solar input.

The effect of radiation penetration on the 24 h average crystal growth is shown in Figure 8, where it can be seen that there is a significant amount of growth near the surface without any solar radiation, just due to the sinusoidal surface temperature. However, it is also clear that, just below the surface, the growth rate increases strongly with increasing radiation penetration. This growth suggests that, for typical values of solar radiation penetrating mid-latitude snow covers, the growth rate just below the surface could be much greater than it is at the snow–soil interface. It also shows that below about 0.15 m depth the growth rate is decreased by radiation penetration. While sub-surface layers of large faceted crystals are commonly observed in polar and high-altitude snow covers, they are not so comon in low-altitude snow covers, thus suggesting that I have overestimated this effect. Perhaps this theory estimates the effect correctly but there are not typically enough days of clear skies to sustain the high rate of sub-surface growth suggested by Figure 8. The growth at the base of the snow cover would proceed as suggested in Figure 8 whether or not cloudy skies interrupt the strong variations at the surface.

A similar effect can be seen in Figure 9, where it is shown that there would be accelerated growth just below the surface due to penetrating radiation, even in the absence of a diurnal cycle in surface temperature (a = 0). The rate of growth increases with the amplitude of the temperature cycle, as would be expected, again suggesting a very strong effect only near the surface.

High-altitude snow cover

I assume the incident radiation penetration is stronger and the temperature cycles are more intense than in seasonal snow covers. This is particularly true in the highest mountains, which occur at low latitudes. In a deep glacial snow cover the temperature and temperature-gradient profiles would be similar to those shown in Figures 3b and 4 because the temperature gradient away from the surface would be very small. Accordingly, at depth the average of the absolute value of the temperature gradient would go to zero instead of the values of 0.15 °C/m assumed in Figures 6 and 7. Therefore, the growth rate would also go to nearly zero below the surface zone of about 0.5 m. The value of b could be around 126 W/m² for high altitudes and the value of a as high as 20 °C. Thus, it is clear that there would be a very large growth rate in a layer of up to 0.1 m depth. These layers are often observed in the spring on south-facing slopes (LaChapelle, 1970) so the process is referred to as "radiation recrystallization", because of the role that both short- and long-wave radiation have in producing the large temperature cycles and sub-surface heating.

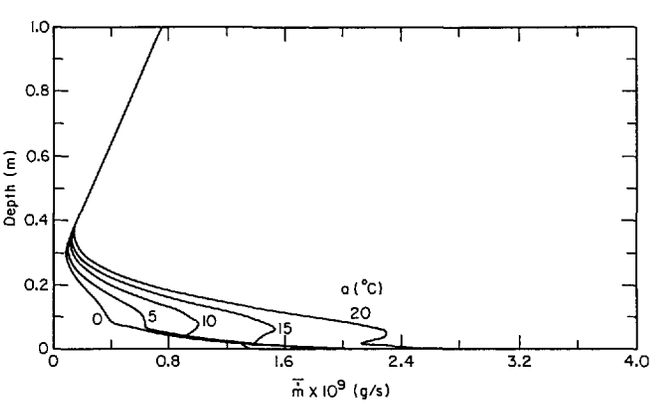

Fig. 9. Profiles of the daily average of the crystal-growth rate for various values of the amplitude (a) of the surface-temperature variation.

Polar ice-sheet snow

Layers of hoar-type crystals have often been reported near the surface of polar ice sheets (Mosley-Thompson and others, 1985; Alley, 1988). Because of the reduced intensity of solar radiation and the large amplitude of the seasonal temperature variation, it seems safe to assume that the formation of hoar crystals arises from the extreme temperature change and that radiation penetration has rather little to do with the problem. However, I will show that this is not true. Since I am now dealing with a seasonal wave which penetrates more deeply than the diurnal wave, the density profile should be considered but it was not included in the original equation. This does place a limit on the value of the results but some general conclusions can be made anyway. If the density were allowed to increase with depth, it would reduce the effect of radiation penetration at depth; the temperature increase at depth would be less than suggested in Figure 10 and the layer of rapid growth would be more concentrated near the surface than is shown in Figure 12. This density effect would be somewhat decreased

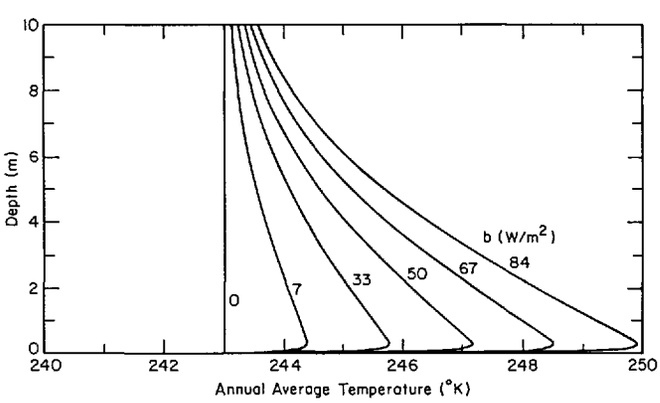

Fig. 10. Annual average temperature profiles for various solar inputs to polar snow.

because the extinction coefficient would decrease as grain-size increases with depth. However, the dominant effect, the increased thermal conductivity due to increased density, is discussed later.

The average annual temperature profile is shown in Figure 10 for various values of radiation penetrating the surface. Using 33 W/m², which is a fairly high value for the polar regions, I found that the temperature rise is about 3 K at 0.2 m, which seems negligible at these low temperatures. The effect of this rise on crystal-growth rate is much greater at higher temperatures but it is also important here. Figure 11 shows how the crystal-growth rate at 0.2 m depth varies throughout the year for varying amounts of penetrating solar radiation. If 33 W/m² is a realistic value, the penetrating radiation doubles the growth rate over what would result from temperature cycling alone. These growth rates are somewhat lower than what was calculated for the seasonal snow cover because of the reduced temperatures. Even so, the total growth in polar snow may be greater because of the longer time available for growth. Most of the growth occurs in the late summer to early fall because of the coincidence of higher temperatures and higher temperature gradients; the peak growth rate occurs between the peak of the temperature and the peak of the temperature gradient at this depth. Growth during the winter is reduced because of the low

https://doi.org/10.3189/002214389793701536 Published online by Cambridge University Press

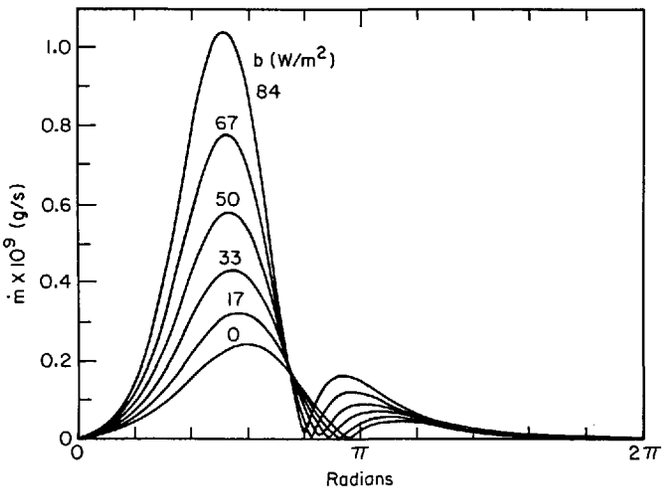

Fig. 11. Distribution of crystal-growth rate at 0.2 m depth in polar snow through an annual cycle for various solar inputs.

temperatures, even though the temperature gradient goes through a large peak. This corresponds to the observation (Alley, 1988) that depth hoar in polar snow develops in late summer to autumn.

The reduction of growth rate with depth is large because of the larger temperature gradients and higher temperatures just below the surface. Figure 12 shows a rapid decay with depth in polar snow as was shown earlier in Figures 8 and 9; thus, if depth hoar forms, I would expect it to form close to the surface. This particular example shows a layer of high growth rate at 0.2–0.3 m depth, but the most rapid growth rate is shown to be adjacent to the surface. In fact, the local density variations would partly control the distribution of depth hoar, but near-surface formation seems to be the rule (Gow, 1965; Mosley-Thompson and others, 1985). Alley (1988) has reported that well-developed depth hoar annually forms at less than 0.2 m depth.

DISCUSSION

I have shown that the amount of solar radiation absorbed beneath the surface of a snow cover can introduce more energy into the snow than can be readily conducted away. Therefore, the sub-surface temperature increases over what it would be in the absence of solar input. The resulting increases in temperature and temperature gradient both contribute to increases in the crystal-growth rate to form sub-surface layers of large, faceted crystals. There would be a high growth rate without the solar input, just because of the large temperature cycles, but solar input definitely increases the sub-surface growth rate. If snow were more conductive or less absorbing, the layer of enhanced temperature would be much less pronounced. This is shown in Figure 13 where the profiles of average daily temperature are shown for pure ice, bubbly ice, and snow. While the effect of penetrating radiation is clear for snow, the effect is very small for bubbly ice and slightly reversed for pure ice. For snow (λ = 20/m), the *e*-folding distance, or 1/*e* decay depth, is 0.05 m and essentially all of the radiation is absorbed in 0.5 m. For bubbly ice, the absorption coefficient is 5/m (personal communication from D. Perovich, U.S. Army CRREL), so that 88% of the energy is absorbed in 0.5 m, but the thermal conductivity is about 80% that of ice, according to the Schwerdtfeger

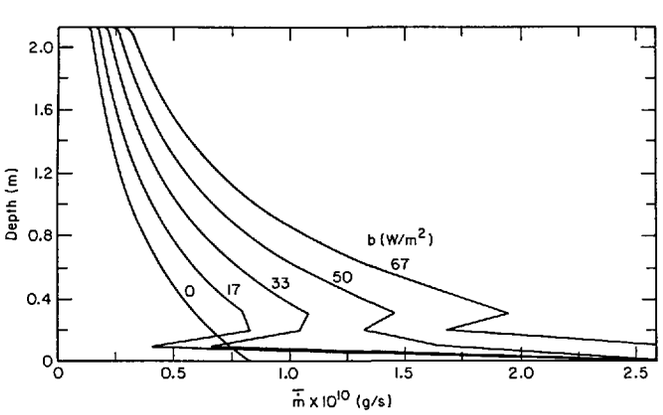

Fig. 12. Profiles of annual average growth rate in polar snow for various solar inputs.

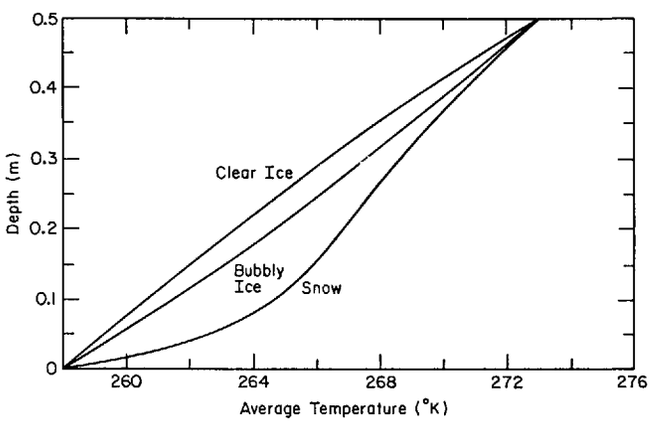

Fig. 13. Profiles of daily average temperature for snow, bubbly ice, and clear ice.

TABLE I. PARAMETERS USED IN FIGURES

Figure	*Period*	*a*	*b*	*ρ*	*k*	$\bar{T}'$	$\bar{T}$	λ	*Material*
		°C	W/m²	Mg/m³	W/m°C	°C/m	K	m⁻¹	
1	24 h or 1 year	–	–	–	–	–	–	–	Snow
2	24 h	15	84	0.3	0.21	10	250	20	Snow
3a	24 h	15	0	0.3	0.21	0	258	20	Snow
3b	24 h	15	140	0.3	0.21	0	258	20	Snow
4	24 h	15	140	0.3	0.21	0	258	20	Snow
5	24 h	15	varies	0.3	0.21	15	258	20	Snow
6	24 h	15	varies	0.3	0.21	15	258	20	Snow
7	24 h	varies	84	0.3	0.21	15	258	20	Snow
8	24 h	10	varies	0.3	0.21	15	258	20	Snow
9	24 h	varies	84	0.3	0.21	15	258	20	Snow
10	1 year	20	varies	0.3	0.21	0	243	20	Snow
11	1 year	20	varies	0.3	0.21	0	243	20	Snow
12	1 year	20	varies	0.3	0.21	0	243	20	Snow
13	24 h	15	84	0.3	0.21	30	258	20	Snow
13	24 h	15	84	0.85	2.00	30	258	5	Bubbly ice
13	24 h	15	84	0.917	2.24	30	258	0.5	Clear ice

https://doi.org/10.3189/002214389793701536 Published online by Cambridge University Press

(1963) formula. Although most of the energy is absorbed fairly quickly, the high thermal conductivity allows it to be conducted away more readily so that the energy does not accumulate in the ice. For clear ice, the effect is even more pronounced, since clear ice (Grenfell and Perovich, 1981) is less absorbing ($\lambda = 0.5$/m) and more conductive. For clear ice, only 22% of the radiation would be absorbed in 0.5 m. Thus, the effect of radiation penetration on ice is very much less than it is on snow. If this were not true, lake ice might "candle", or melt by internal radiation absorption just below the surface on cool, clear days.

While radiation penetration increases the average temperature and temperature gradient just below the surface in snow, it decreases the average temperature gradient in an intermediate layer below that. The effect of this is to decrease the growth rate in that intermediate layer as shown in Figure 8. This layer of smaller crystals would serve to highlight to an observer the presence of a layer of rapidly growing crystals in the near-surface layer. The entire column is heated as shown in Figure 5, not because of radiation absorption at greater depth but because of reduced heat conduction up through the snow at that depth. The amount of solar radiation reaching 0.5 m depth in snow is not in itself sufficient to explain the temperature increase shown in that example.

CONCLUSION

Profiles of temperature, temperature gradient, and crystal-growth rate have been shown for a sinusoidally varying surface temperature with solar-radiation input during one-half of the period. Layers of faceted crystals observed to grow just below the surface of high-altitude snow covers and polar snow are explained by the combination of the high temperature gradients associated with the periodic surface temperature, and the increased temperature and temperature gradients due to solar radiation input. These layers could occur with either radiation input or temperature cycling, but the growth rate increases with both solar input and the magnitude of the temperature cycle. In most cases, the growth rate has a relative peak in a layer 0.05–0.1 m below the surface for a seasonal snow cover, or 0.2–0.3 m below the surface in polar snow. The highest growth rates are calculated to be adjacent to the surface, but growth in these layers would be strongly affected by the close proximity of the atmospheric vapor sink.

The growth rates predicted for polar snow are reasonable, although the quantitative results of these calculations are questionable since the geometry of the snow has not been adequately represented and Equation (14) needs further experimental testing. The growth rates calculated for the seasonal snow cover and shown in Figures 8 and 9 indicate that the growth rate in the near-surface layer at 0.05–0.1 m would be as high under some conditions (e.g. $a = 10\,^{\circ}\mathrm{C}$ and $b = 63\ \mathrm{W/m^2}$) as the growth rate at the warmer base of the snow cover. This result may be correct, although these near-surface layers are not usually seen in the seasonal snow cover, possibly because of the lack of enough sequential days of cold, clear weather or the loss of vapor to the atmosphere due to wind-pumping. They are seen in high-altitude snow covers because of the extreme radiational balances.

ACKNOWLEDGEMENTS

This work was suggested by R. Berger's concern about wet snow layers in an apparently cold snow cover. The inputs of Dr R.B. Alley, Dr D. McClung, and Dr D. Perovich were appreciated. I also appreciated an anonymous reviewer who checked the equations carefully enough to catch some misprints. The work was supported at CRREL by Work Unit 4A161102AT24, Mechanical Processes in a Snow Cover.

REFERENCES

Akitaya, E. and H. Shimizu. 1987. Observations of weak layers in a snow cover. *Low Temp. Sci., Ser. A*, 46, 67-75.

Alley, R.B. 1988. Concerning the deposition and diagenesis of strata in polar firn. *J. Glaciol.*, 34(118), 283-290.

Carslaw, H.S. and J.C. Jaeger. 1959. *Conduction of heat in solids. Second edition.* London, Oxford University Press.

Colbeck, S.C. 1983. Theory of metamorphism of dry snow. *J. Geophys. Res.*, 88(C9), 5475-5482.

Gow, A.J. 1965. On the accumulation and seasonal stratification of snow at the South Pole. *J. Glaciol.*, 5(40), 467-477.

Grenfell, T.C. and D.K. Perovich. 1981. Radiation absorption coefficients of polycrystalline ice from 400–1400 nm. *J. Geophys. Res.*, 86(C8), 7447-7450.

LaChapelle, E.R. 1970. Principles of avalanche forecasting. *In* Gold, L.W. and G.P. Williams, *eds. Ice engineering and avalanche forecasting and control.* Ottawa, National Research Council of Canada. Associate Committee on Geotechnical Research, 106-112. (Tech. Memo. 98.)

Lamb, D. and P.V. Hobbs. 1971. Growth rates and habits of ice crystals grown from the vapor phase. *J. Atmos. Sci.*, 28(8), 1506-1509.

Mosley-Thompson, E., P.D. Kruss, L.G. Thompson, M. Pourchet, and P. Grootes. 1985. Snow stratigraphic record at South Pole: potential for paleoclimatic reconstruction. *Ann. Glaciol.*, 7, 26-33.

Powers, D., K. O'Neill, and S.C. Colbeck. 1985. Theory of natural convection in snow. *J. Geophys. Res.*, 90(D6), 10641-10649.

Schwerdtfeger, P. 1963. The thermal properties of sea ice. *J. Glaciol.*, 4(36), 789-807.

Schytt, V. 1958. Glaciology II. *Norwegian–British–Swedish Antarctic Expedition, 1949–52. Sci. Results*, 4.

Weller, G. and P. Schwerdtfeger. 1977. Thermal properties and heat transfer processes of low-temperature snow. *In* Businger, J.A., *ed. Meteorological studies at Plateau Station, Antarctica.* Washington, DC, American Geophysical Union, 27-34. (Antarct. Res. Ser., 25.)

MS. received 24 May 1988 and in revised form 17 August 1988